1986ApJ...307L..75Z

THE ASTROPHYSICAL JOURNAL, 307:L75–L79, 1986 August 15
© 1986. The American Astronomical Society. All rights reserved. Printed in U.S.A.

OBSERVATIONS OF NEUTRAL ATOMIC CARBON AT 809 GHz

J. ZMUIDZINAS, A. L. BETZ, AND D. M. GOLDHABER
Space Sciences Laboratory, University of California, Berkeley
Received 1986 May 13; accepted 1986 May 23

ABSTRACT

We have detected the 809 GHz $^3P_2$–$^3P_1$ fine-structure line of neutral atomic carbon in four dense molecular clouds: M17, W51, W3, and DR 21(OH). These observations complement the published observations of the 492 GHz $^3P_1$–$^3P_0$ line and allow the excitation temperature of the ^3P levels along with the line optical depths to be determined. The results indicate excitation temperatures $T_x \approx 30$–60 K and optical depths of $\tau_{10} \lesssim 1$. This implies that the $\sim 10^{18}$ cm^{-2} lower limit to the C I abundance derived from 492 GHz observations is probably the actual abundance, which gives C I/CO ≈ 0.1 in dense molecular clouds.

Subject headings: interstellar: abundances — interstellar: matter — nebulae: abundances

I. INTRODUCTION

The ^3P ground state of neutral atomic carbon is split by spin-orbit coupling into the $J = 0$, 1, and 2 levels which have energies of 0 K, 23.6 K, and 62.4 K, respectively. Magnetic dipole transitions are allowed between adjacent levels; these lead to the $^3P_2$–$^3P_1$ transition at 809.3432 GHz (370.4145 μm) and the $^3P_1$–$^3P_0$ transition at 492.1612 GHz (609.1347 μm) (Cooksy *et al.* 1986). The $^3P_1$–$^3P_0$ line has been observed in many dense molecular clouds by Phillips and Huggins (1981), and the spatial distribution of intensity in two clouds has also been presented (Keene *et al.* 1985). The large observed $^3P_1$–$^3P_0$ intensities implied lower limits to the C I column densities ($N_{\rm C\,I} \approx 0.1\ N_{\rm CO}$) which were much larger than the column densities predicted by steady state models of cloud chemistry (Langer 1976*a*), although time-dependent models predicted a large C I abundance for the first 10^6 yr of cloud evolution (Langer 1976*b*). Several other models have since been proposed to explain the high observed abundance (e.g., Tarafdar *et al.* 1985; Tielens and Hollenbach 1985). A good review of the current situation is presented by Keene *et al.* (1985). Phillips and Huggins (1981) have further argued that comparisons between CO and C I line widths imply that the $^3P_1$–$^3P_0$ lines are optically thick, and that the abundance of carbon could be as large as $N_{\rm C\,I} \approx 0.7\,N_{\rm CO}$ in some cases. The largest optical depth derived by this comparison was $\tau_{10} \approx 25$ for OMC-1. The comparison was only carried out for a few clouds which had well-defined CO line width–opacity relationships, but the implication was that the C I lines were possibly optically thick in other clouds as well. A more direct approach for estimating the C I abundance would have been to observe both of the C I fine-structure lines (the $^3P_1$–$^3P_0$ line at 492 GHz and the $^3P_2$–$^3P_1$ line at 809 GHz) and compare the results, but observations at the higher frequency were not possible at the time. The first detection of the $^3P_2$–$^3P_1$ line was subsequently presented by Jaffe *et al.* (1985), who detected it in OMC-1. Although their data favor optically thin C I lines, the result is not firm due to large systematic uncertainties. We have recently observed the $^3P_2$–$^3P_1$ line in four dense molecular clouds: M17, W51, W3, and DR 21(OH). In this *Letter* we present our data, compare them to existing $^3P_1$–$^3P_0$ data, and derive estimates for the excitation temperature and column density of neutral carbon.

II. OBSERVATIONS

Since the transmission of the atmosphere at 370 μm is at best rather poor from the ground, we observed the $^3P_2$–$^3P_1$ transition from the NASA Kuiper Airborne Observatory (KAO) at an altitude of 41,000 feet. The observations were completed in 1985 July using an airborne far-infrared heterodyne receiver (Betz and Zmuidzinas 1984). This is the first laser spectrometer to be used aboard the KAO, although similar (but larger) instruments have been used at ground-based observatories (e.g., Koepf *et al.* 1982; Jaffe *et al.* 1985). Briefly, it consists of a CO_2 laser-pumped far-infrared laser local oscillator (LO), a polarization diplexer to combine telescope and LO beams, and a GaAs Schottky diode mixer in an open structure mount. A velocity resolution of 1.85 km s^{-1} over an interval of 74 km s^{-1} was achieved by using a filter bank with 40 5 MHz channels to analyze the intermediate frequency (IF) signal. The room-temperature receiver had a 20,000 K (SSB) noise temperature.

We used the chopping secondary of the telescope to switch between two beams that were alternately placed on the source. At the chopping frequency of 21 Hz the maximum chopper-throw consistent with a reasonable waveform efficiency was 5′, which in some cases may not have been sufficient to place the off-source beam in a region free of emission (see § IV). The absolute flux calibration was derived from raster scans of the telescope beam across Jupiter. The calibration uncertainty is dominated by source coupling effects, as will be discussed in § IV. These measurements, corrected for the finite size of Jupiter, also provided the beam size (80″ FWHM), the main beam efficiency ($\sim$ 30% including chopper waveform inefficiency), and the instrument boresight (to $\pm15''$). We assumed that Jupiter had an uniform elliptical intensity distribution with major and minor axes of 48″ and 45″, respec-

© American Astronomical Society • Provided by the NASA Astrophysics Data System

1986ApJ...307L..75Z

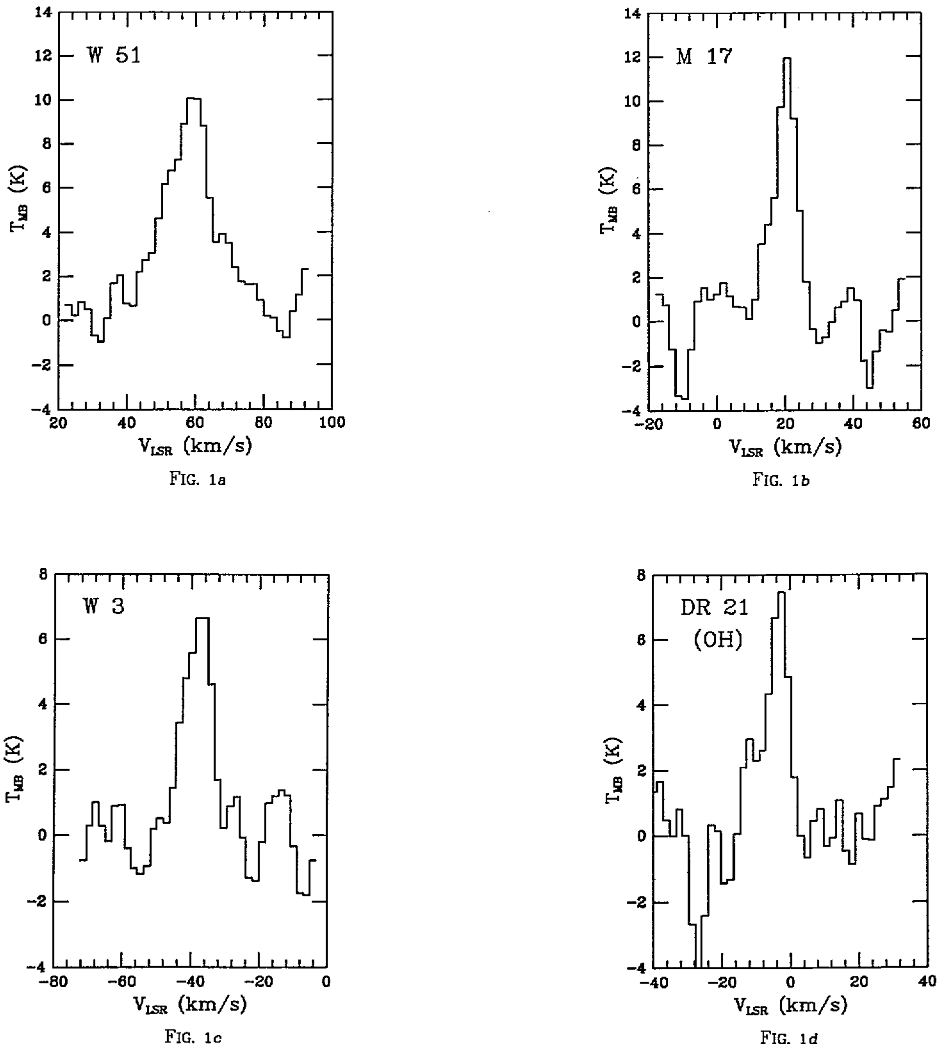

FIG. 1.—809 GHz C I $^3P_2$–$^3P_1$ emission observed toward (*a*) W51, integration time = 32 minutes; (*b*) M17, integration time = 44 minutes; (*c*) W3, integration time = 58 minutes; and (*d*) DR 21(OH), integration time = 23 minutes.

tively, and a brightness temperature of 160 K at 370 μm (Hildebrand *et al.* 1985). The Moon, which was used to calibrate the $^3P_1$–$^3P_0$ data (Phillips and Huggins 1981), was not available at the time of these observations. The overall pointing accuracy is estimated to be between 20″ and 30″.

III. RESULTS

Figures 1*a*–1*d* show the $^3P_2$–$^3P_1$ spectra measured for four dense clouds: M17, W51, W3, and DR 21(OH). The observed positions were chosen to match locations where $^3P_1$–$^3P_0$ emission had been measured previously. We also observed S140 but failed to detect a line. The $^3P_1$–$^3P_0$ emission in S140 has been shown to have a spatial extent of over 10′ in a direction similar to our misoriented chop direction (Keene *et al.* 1985). Consequently, emission in the reference beam may have canceled equivalent emission in the "on-source" beam to produce a zero differential signal. If this is so, then the $^3P_2$–$^3P_1$ emission and the $^3P_1$–$^3P_0$ emission have similar spatial distributions.

The spectra in Figure 1 have been Hanning smoothed to an effective resolution of 3.7 km s^{-1}, and small linear baselines have been subtracted. Table 1 shows the measured peak intensities, line widths, line centers, and their uncertainties. These parameters were determined by fitting a Gaussian profile degraded by the instrumental resolution to the unsmoothed data, in order to correct these parameters for the finite resolution of the spectrometer. The χ^2 values of the fits were consistent with independent measurements of the receiver noise, although the line profiles are not necessarily expected to be Gaussian (the *S/N* ratio is not large enough to show the fine details of the line profile). Also shown in Table 1 are $^3P_1$–$^3P_0$ line parameters. The center velocities agree well, while the line widths agree well only for M17 and DR 21(OH). We expect the line widths to be similar if the gas is optically thin, while the $^3P_1$–$^3P_0$ line should be somewhat wider than the $^3P_2$–$^3P_1$ line if the gas were cool and optically thick since the optical depth of the $^3P_1$–$^3P_0$ line would be ~ 2 times larger than the depth of the $^3P_2$–$^3P_1$ line (for

© American Astronomical Society • Provided by the NASA Astrophysics Data System

1986ApJ...307L..75Z

TABLE 1

C I LINE PARAMETERS

Source	T_{MB}(2–1) (K)	ΔV(2–1) (km s^{-1})	V_{center}(2–1) (km s^{-1})	T_A^*(1–0) (K)	ΔV(1–0) (km s^{-1})	V_{center}(1–0) (km s^{-1})
M17[a]	12.9 ± 1.3	6.7 ± 0.8	19.6 ± 0.7	11.0	6.4	20.5
W51[b]	8.9 ± 1.0	16.0 ± 2.2	57.5 ± 1.0	8.0	20.5	60.0
W3[b,c]	7.3 ± 0.9	9.1 ± 1.5	−38.8 ± 0.8	6.0	5.0	−38.0
DR 21(OH)[d]	8.5 ± 1.9	5.7 ± 1.5	−4.0 ± 0.8	4.0	5.0	...

NOTE.—The quoted uncertainties are $\pm 1\ \sigma$.

[a] 1–0 data from Keene *et al.* 1985.

[b] 1–0 data from Phillips and Huggins 1981.

[c] The value shown in Table 1 of Phillips and Huggins 1981 for the 1–0 line width is 6.5 km s^{-1}. However, their published spectrum shows a line width of 5 km s^{-1} (FWHM). We believe the larger value to be a typographical error.

[d] 1–0 data from J. Keene 1986, private communication.

$T_x \approx 20$ K). However, the line width variations are probably best explained by the fact that the two different beams (80″ at 809 GHz versus 180″ at 492 GHz) sample different spatial regions of sources with a complex velocity structure (Phillips *et al.* 1981; Brackmann and Scoville 1980 [W3]; Mufson and Liszt 1979 [W51]).

IV. INTENSITY CALIBRATION AND SOURCE COUPLING EFFECTS

A comparison of the intensities of the $^3P_2$–$^3P_1$ and $^3P_1$–$^3P_0$ transitions can provide useful information about the abundance and excitation of carbon. However, the comparison of intensities is not straightforward since the beam size of the $^3P_1$–$^3P_0$ observations (3′) is a factor of 2 larger than that of the $^3P_2$–$^3P_1$ observations, and so the source coupling differs. Furthermore, the calibration procedures (and sources) differ. These details are important in interpreting the data since the $^3P_2$–$^3P_1$/$^3P_1$–$^3P_0$ line intensity ratio for optically thin gas is at most only a factor of 2 larger than the same ratio for optically thick gas. In fact, the source-coupling corrections change the line intensities by $\sim 30\%$ or more; hence, the statistical uncertainties in the data ($\sim 15\%$) are small compared to the uncertainties in the source coupling.

The $^3P_1$–$^3P_0$ data were calibrated in such a manner that a source of uniform intensity T_R(1–0) filling the entire diffraction pattern of the telescope, including sidelobes, would give a measured intensity of $T_A^*(1–0) = T_R(1–0)$. A source not large enough to fill all of the sidelobes completely would give $T_A^*(1–0) = \eta_{1-0} T_R(1–0)$, where $\eta_{1-0} < 1$ (Kutner and Ulich 1981). On the other hand, the $^3P_2$–$^3P_1$ data were calibrated in such a manner that a source of uniform intensity T_R(2–1) filling only the main lobe of the diffraction pattern and not filling any sidelobes would give a measured intensity of $T_{MB}(2–1) = T_R(2–1)$. If the source were smaller than the main lobe the measured intensity would be $T_{MB}(2–1) = \eta_{2-1} T_R(2–1)$ with $\eta_{2-1} < 1$, while if the source were larger than the main lobe and started filling the sidelobes as well, we would have $\eta_{2-1} > 1$. We calculated both of these source coupling coefficients, η_{1-0} and η_{2-1}, assuming a Gaussian source intensity distribution with a peak intensity T_R and a theoretically calculated telescope diffraction pattern. The results are plotted in Figure 2 as a function of assumed source size.

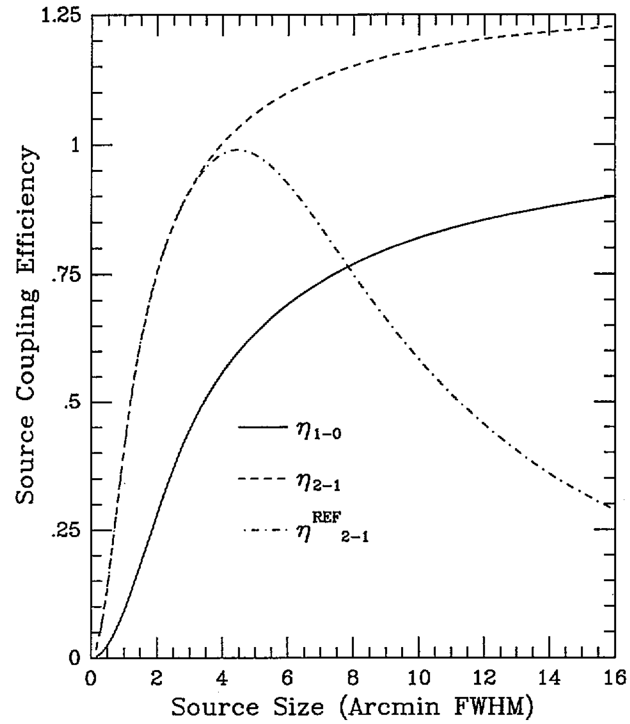

FIG. 2.—*Solid line*: source coupling efficiency η_{1-0} for the $^3P_1$–$^3P_0$ observations as a function of source size. *Dashed line*: source coupling efficiency η_{2-1} for the $^3P_2$–$^3P_1$ observations. *Dot-dashed line*: η_{2-1} corrected for emission in the reference beam.

The difference between the two calibrations is easily understood by considering the calibration sources used. The $^3P_1$–$^3P_0$ data were calibrated by using the Moon, which fills the entire telescope diffraction pattern, while the $^3P_2$–$^3P_1$ data were calibrated using Jupiter, which fills only a small fraction of the main lobe of the diffraction pattern. The main lobe was scanned across Jupiter in order to deduce the strength of the signal that would have been measured on a source large enough to fill the main lobe. We could not directly deduce the

© American Astronomical Society • Provided by the NASA Astrophysics Data System

1986ApJ...307L..75Z

TABLE 2

OPTICAL DEPTHS AND EXCITATION TEMPERATURES

Source	A: Uncorrected[a]				B: Corrected[b]				C: Corrected[c]				
	T_x	T_{LL}[d]	τ_{10}	τ_{UL}[e]	T_x	T_{LL}[d]	τ_{10}	τ_{UL}[e]	T_x	T_{LL}[d]	τ_{10}	τ_{UL}[e]	θ_{SOURCE}[f]
M17	72.	53.	0.20	0.31	36.	26.	0.95	> 2	48.	36.	0.56	0.91	6.′2
W51	64.	47.	0.17	0.25	37.	21.	0.51	0.81	64.	46.	0.22	0.37	7.8
W3.....................	74.	51.	0.10	0.17	31.	22.	0.87	> 2	31.	22.	0.83	> 2	3.5
DR 21(OH)...........	> 200.	89.	< 0.03	0.09	98.	44.	0.07	0.20	147.	55.	0.04	0.15	6.0

[a] Derived from measured line intensities with no correction for source coupling effects.
[b] Corrected for source coupling only using a source size of θ_{SOURCE}.
[c] Corrected for source coupling and reference beam emission using a source size of θ_{SOURCE}.
[d] Lower limit for T_x (95% confidence level; based on statistical uncertainty of 2–1 intensity only).
[e] Upper limit for τ_{10} (95% confidence level; based on statistical uncertainty of 2–1 intensity only).
[f] θ_{SOURCE} is the ^{12}CO(1–0) source size (FWHM). The CO source sizes are taken from Thronson and Lada 1983, see also Keene *et al.* 1985 (M17); Mufson and Liszt 1979 (W51); Brackmann and Scoville 1980 (W3); Dickel *et al.* 1978 [DR 21(OH)].

signal that a source filling the entire telescope pattern would have produced because the signal-to-noise ratio was not large enough to allow the sidelobes to be mapped in the available time.

Another important consideration for the $^3P_2$–$^3P_1$ data is the possibility that the 5′ chopper throw was not large enough, and that there was emission from the source in the reference beam, which would cause the differential signal to be smaller. This effect obviously depends on source size. We define η_{2-1}^{REF} to be the ratio $T_{MB}(2–1)/T_R(2–1)$ corrected for reference beam emission, again assuming a Gaussian source intensity distribution, and we plot it in Figure 2 as a function of source size.

V. DISCUSSION

We model the measured C I line intensities with an emission region of uniform temperature in which the ^3P levels are fully thermalized [$n(H_2) \geq 10^4$ cm^{-3}]. We also assume that the velocity distribution of the gas sampled with the 180″ beam at 492 GHz is similar to the velocity distribution of the gas sampled with the 80″ beam at 809 GHz, although this assumption probably breaks down for W3, as shown by the line widths in Table 1. Only two unknown quantities, the $^3P_1$–$^3P_0$ line optical depth at the center velocity $\tau_{10}(V_{center})$ and the excitation temperature T_x, determine the line intensities in this model, so a measurement of the two intensities allows us to fully determine these parameters. Other parameters of interest, namely the $^3P_2$–$^3P_1$ optical depth τ_{21} and the C I column density $N_{C\ I}$, can be derived assuming thermal equilibrium. Under such circumstances, the ratio of optical depths τ_{21}/τ_{10} is larger than 1 for $T_x > 50$ K and asymptotically approaches the value of 2.1 as T_x is increased, while τ_{21}/τ_{10} is less than 1 for $T_x < 50$ K.

We derive T_x and τ_{10} for three sets of line intensities. The first set A is given by $T_R(1–0) = T_A^*(1–0)$ and $T_R(2–1) = T_{MB}(2–1)$; here we take the line intensities "as is" and perform no corrections. The second set B is given by $T_R(1–0) = T_A^*(1–0)/\eta_{1-0}$ and $T_R(2–1) = T_{MB}(2–1)/\eta_{2-1}$. The source sizes used in estimating the source coupling coefficients are listed in Table 2 (see Fig. 2 also) and are derived from maps of $J = 1 \rightarrow 0$ ^{12}CO emission. Scans of the C I $^3P_1$–$^3P_0$ emission in OMC-1 (Phillips and Huggins 1981), and M17 and S140 (Keene *et al.* 1985), indicate that the C I emission region is similar in extent to the CO emission region, and, as mentioned in § III, our nondetection of $^3P_2$–$^3P_1$ emission in S140 may provide evidence that the $^3P_2$–$^3P_1$ emission and the $^3P_1$–$^3P_0$ emission have similar spatial distributions. The third set C of intensities for which we calculate T_x and τ_{10} is the same as the second set with η_{2-1} replaced by η_{2-1}^{REF}; this attempts to correct for possible emission in the reference beam. The corresponding values of T_x and τ_{10} are listed in Table 2. The results show that $\tau_{10} < 1$ in all cases, and that T_x is typically 30–60 K. M17 and W3 show the largest corrected optical depths; for M17 this is due to the large observed $^3P_1$–$^3P_0$ intensity, while for W3 this is due to the large upward correction to the observed $^3P_1$–$^3P_0$ intensity necessitated by its small 3.′5 source size. Both W51 and DR 21(OH) appear to be optically thin regardless of the assumed correction. In the case of DR 21(OH) the excitation temperatures seem anomalously high. However, the $^3P_2$–$^3P_1$ intensity has a large uncertainty, as indicated by the considerably smaller lower limits for T_x shown in Table 2.

Since the lines seem to be optically thin, the lower limits to the column densities of C I ($\sim 10^{18}$ cm^{-2}), derived by Phillips and Huggins (1981) using an optically thin approximation with $T_x = 20$ K, are likely to be the actual column densities. The column densities derived in this approximation are very insensitive to the assumed excitation temperature, changing by only 25% over the range 15 K $\leq T_x \leq$ 200 K. The minimum column densities are calculated by assuming $T_x = 30$ K, while the column densities calculated by assuming $T_x = 20$ K are only 6% larger. After correction for source coupling (case B above), we derive the following column densities (in units of 10^{18} cm^{-2}): 2.1 for M17, 2.8 for W51, 2.1 for W3, and 0.5 for DR 21(OH). Note that these are the peak column densities; the column densities averaged over the source or averaged over a beam would be smaller.

If we compare the parameters derived from the uncorrected line intensities to the parameters derived from the intensities corrected for source coupling, we see that the source-corrected excitation temperatures drop typically by a factor of 2, while

© American Astronomical Society • Provided by the NASA Astrophysics Data System

1986ApJ...307L..75Z

the optical depths increase by an even larger factor. This demonstrates the sensitivity of the results to the assumed source-coupling coefficients, especially to the large upward corrections of the $^3P_1$–$^3P_0$ intensities. However, the source-coupling coefficients are derived with the aid of several assumptions and are not known precisely. Hence, it is difficult to put strict upper limits on the derived values of τ_{10} or lower limits on T_x, especially for M17 and W3. The solution to this problem, of course, is to use beam sizes that are much smaller than the source size (such as would be obtained from a larger telescope), and to make sure that the source positions and reference positions are well separated. Even with a 30% relative uncertainty between the two intensities, firm limits could be placed on the model parameters. Future observations of isotopic C I may also help to reduce uncertainties in the estimates of the optical depths.

We thank the staff of the Kuiper Airborne Observatory for their expert assistance with this new project. We are grateful to J. Keene for communicating C I $^3P_1$–$^3P_0$ results prior to publication, and to her and D. Jaffe for many helpful discussions. This work was supported in part by NASA grant NAG 2-254.

REFERENCES

Betz, A., and Zmuidzinas, J. 1984, in *Proc. Airborne Astronomy Symposium* (NASA CP-2353), p. 320.
Brackmann, E., and Scoville, N. 1980, *Ap. J.*, **242**, 112.
Cooksy, A. L., Saykally, R. J., Brown, J. M., and Evenson, K. M. 1986, *Ap. J.*, in press.
Dickel, J. R., Dickel, H. R., and Wilson, W. J. 1978, *Ap. J.*, **223**, 840.
Hildebrand, R. H., Lowenstein, R. F., Harper, D. A., Orton, G. S., Keene, J., and Whitcomb, S. E. 1985, *Icarus*, **64**, 64.
Jaffe, D. T., Harris, A. I., Silber, M., Genzel, R., and Betz, A. L. 1985, *Ap. J.* (*Letters*), **290**, L59.
Keene, J., Blake, G. A., Phillips, T. G., Huggins, P. J., and Beichman, C. A. 1985, *Ap. J.*, **299**, 967.
Koepf, G. A., Buhl, D., Chin, G., Peck, D. D., Fetterman, H. R., Clifton, B. J., and Tannenwald, P. E. 1982, *Ap. J.*, **260**, 584.
Kutner, M. L., and Ulich, B. L. 1981, *Ap. J.*, **250**, 341.
Langer, W. 1976*a*, *Ap. J.*, **206**, 699.
______. 1976*b*, *Ap. J.*, **210**, 328.
Mufson, S. L., and Liszt, H. S. 1979, *Ap. J.*, **232**, 451.
Phillips, T. G., and Huggins, P. J. 1981, *Ap. J.*, **251**, 533.
Phillips, T. G., Knapp, G. R., Huggins, P. J., Werner, M. W., Wannier, P. G., Neugebauer, G., and Ennis, D. 1981, *Ap. J.*, **245**, 512.
Tarafdar, S. P. Prasad, S. S., Huntress, W. T., Villere, K. R., and Black, D. C. 1985, *Ap. J.*, **289**, 220.
Thronson, H. A., and Lada, C. J. 1983, *Ap. J.*, **269**, 175.
Tielens, A. G. G. M., and Hollenbach, D. 1985, *Icarus*, **61**, 40.

Note added in proof.—An analysis of recent observations of the $^3P_1$–$^3P_0$ line in DR 21(OH) (J. Keene 1986, private communication) indicates a peak antenna temperature T_A^* (1–0) of 6.5 K, which is 50% higher than the preliminary value given in Table 1. This larger intensity results in excitation temperatures T_x of 86, 41, and 52 K for cases A, B, and C in Table 2, along with optical depths τ_{10} of 0.09, 0.36, and 0.26, respectively. The upper limit to the optical depth of the $^3P_1$–$^3P_0$ line is $\tau_{UL} = 0.95$ for case B. The new values are similar to those derived for the other three observed sources.

A. L. Betz, D. M. Goldhaber, and J. Zmuidzinas: Space Sciences Laboratory, University of California, Berkeley, CA 94720

© American Astronomical Society • Provided by the NASA Astrophysics Data System